# Chapter 7

# Effects of Small-Scale Galactic Structure on Streams

We saw in the previous chapter that in addition to their (relatively) predictable internal dynamics, streams are shaped by large features of the Galactic potential such as its bar. With a solid understanding of all of these effects, we can begin to tease out perturbations to streams from small scale structure in the galaxy, including other clusters, giant molecular clouds, and of course, dark matter subhalos. **These perturbers interact with streams as they orbit, leaving observable signatures in their density and kinematic structure**. At the highest level, a perturber passing close to the stream imparts a velocity kick to the stars at the impact site, changing their orbits to either produce and underdensity/gap (if the impactor is massive and/or the interaction is very close, where multiple close encounters may cause multiple gaps), or to dynamically heat the stream (if the impactor is lower mass and/or at a larger distance from the stream). Our study of low-mass structure using streams comes in two flavors: (1) inferring the properties of individual perturbers from specific features in streams and (2) inferring the population of perturbers based on the effect of their accumulated impacts over the stream's lifetime. We will begin by discussing the former.

The following theory papers (motivated by clumpy structures discovered in early observations of GC stream density profiles alongside the "missing satellite problem" for CDM) are typically all cited after statements like the bolded sentence above: Ibata et al. (2002); Johnston et al. (2002); Carlberg (2009); Yoon et al. (2011); Erkal & Belokurov (2015a,b); Erkal et al. (2016b). We will attempt to complement review of this work with more recent observational efforts, made possible with *Gaia* astrometry and radial velocity spectroscopy, as the field moves toward a more complete 6D phase space picture of Milky Way streams.

## 7.1 Individual stream/perturber interactions

Here we will follow the derivations of Erkal & Belokurov (2015a); their problem setup is shown in Figure 7.1. A stream is modeled as a straight line of stars a distance $r_0$ from the Galactic center and orbiting in the disk at the circular velocity $v_y = \sqrt{r_0 \partial_r \phi(r_0)}$ (where $\phi$ is the Galactic potential; recall that its gradient gives the gravitational acceleration, equation 2.3). A perturber has velocity $\overline{w} = (w_x, w_y, w_z) = (w_\perp \sin\alpha, w_y, w_\perp \cos\alpha)$, where $w_\perp = \sqrt{w_x^2 + w_y^2}$. The relative velocity between the subhalo and the stream in the $y$ direction (that is, along the stream's motion) is $w_\parallel = v_y - w_y$. The magnitude of the perturber's relative velocity to the stream is $w = \sqrt{w_\parallel^2 + w_\perp^2}$. The closest approach occurs in the $x$-$z$ plane at $y = 0$ with impact parameter $b = \sqrt{b_x^2 + b_z^2}$.

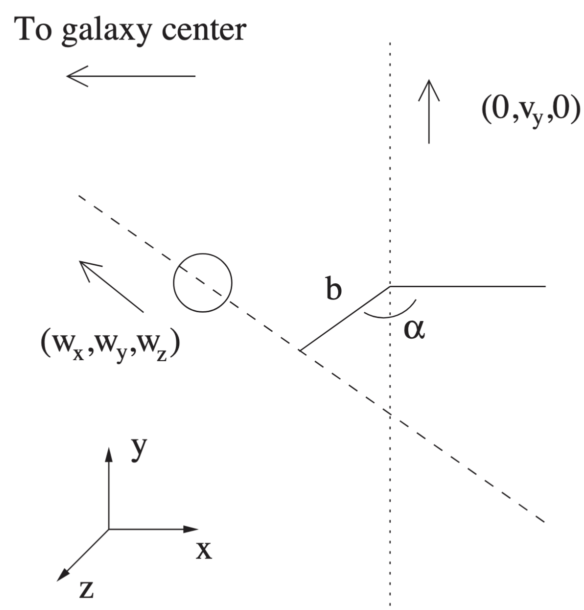


**Figure 7.1:** From Erkal & Belokurov (2015a), the configuration of the modeled stream-perturber interaction.

We will let the subhalo be modeled here by a Plummer sphere of mass $M$ and scale radius $r_s$. The velocity kick to stream particles does not exactly generalize to any spherical subhalo, but the qualitative behavior is captured accurately here for any subhalo potential characterized by a mass and scale radius (see Erkal & Belokurov 2015a, §6.1). We will neglect differential velocities of the stream stars prior to the interaction, so that all stream stars have initial velocity $v_y$. The passing perturber imparts a velocity kick $\Delta v$ to the stream particles, where we assume that $\Delta v \ll v_{stream}$. In this limit, we can apply the **impulse approximation** (as introduced in Chapter 2). For the kick toward/away from the Galactic center:

$$\begin{aligned} \Delta v_x &= \int_{-\infty}^{\infty} a_x dt \\ &= \int_{-\infty}^{\infty} \frac{GM(b_x + w_x t)}{\left[(y + w_\parallel t)^2 + w_\perp^2 t^2 + b^2 + r_s^2\right]^{3/2}} dt \\ &= \frac{2GM(bw^2 \cos\alpha + y w_\perp w_\parallel \sin\alpha)}{w[(b^2 + r_s^2)w^2 + w_\perp^2 y^2]}. \end{aligned} \tag{7.1}$$

There are many terms in this equation, given the generalization of the impulse approximation to 3 dimensions, as well as the accounting for the distance of the perturbed stars along the stream from the impact site, $y$. Nonetheless, we see analogous terms in the integrand $a_x$ to the perpendicular acceleration given in Equation 2.10. Not too scary. If we let $\psi$ be the longitidue coordinate along the stream (so that the distance along the stream $y = r_0\psi_0$) and use the perturber velocity components along $x$, $y$, and $z$ to eliminate the angle $\alpha$, we find

$$\Delta v_x(\psi_0) = \frac{2GM}{r_0^2 w_\perp^2 w} \frac{(bw^2 \frac{w_z}{w_\perp} - \psi_0 r_0 w_\parallel w_x)}{\psi_0^2 + \frac{(b^2+r_s^2)w^2}{r_0^2 w_\perp^2}} \tag{7.2}$$

We can similarly compute the velocity kick along the stream (along $y$) and and along the $z$ axis, finding

$$\begin{aligned} \Delta v_y &= -\frac{2GMw_\perp^2 y}{w[(b^2 + r_s^2)w^2 + w_\perp^2 y^2]} = -\frac{2GM\psi_0}{wr_0\left(\psi_0^2 + \frac{(b^2+r_s^2)w^2}{r_0^2 w_\perp^2}\right)} \\ \Delta v_z &= \frac{2GM(bw^2 \sin\alpha - y w_\perp w_\parallel \cos\alpha)}{w[(b^2 + r_s^2)w^2 + w_\perp^2 y^2]} = -\frac{2GM}{r_0^2 w_\perp^2 w} \frac{(bw^2 \frac{w_x}{w_\perp} - \psi_0 r_0 w_\parallel w_z)}{\psi_0^2 + \frac{(b^2+r_s^2)w^2}{r_0^2 w_\perp^2}}. \end{aligned} \tag{7.3}$$

Again, many terms to keep track of! Figure 7.2 shows the qualitative behavior of the velocity kick along the stream, highlighting the infamous "1/x" velocity signature imparted immediately after the flyby. A high-amplitude signal is achieved by a small relative velocity (with a comparatively large fraction of the velocity directed perpendicularly to the stream's motion), a small impact parameter, and a massive and/or compact perturber.

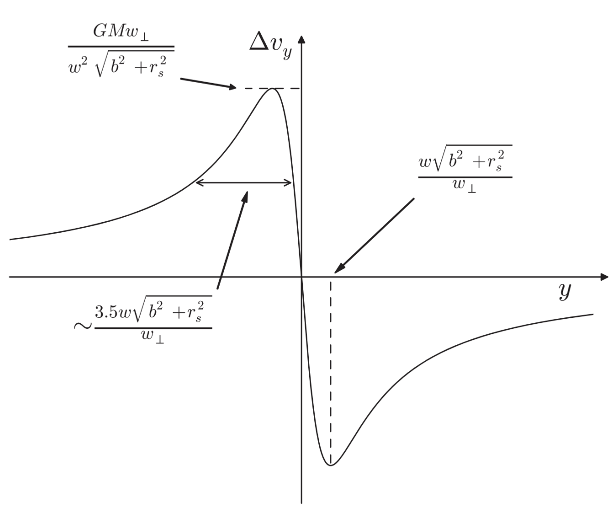


**Figure 7.2:** From Erkal & Belokurov (2015a), the velocity kick along a stream immediately following a perturber flyby.

With the velocity kicks $(\Delta v_x, \Delta v_y, \Delta v_z)$ in hand, we can compute the orbit of each particle along the stream. We keep around only leading order terms in $\Delta v/v_y$, and ignore the kick along $z$ for now, as it causes oscillatory rather than secular motion (although, see below). We can describe the dependence of a particle's radius on its orbital phase $\theta$ as

$$\frac{d^2u}{d\theta^2} + u = -\frac{1}{L_z^2}\partial_u\phi, \tag{7.4}$$

where we have changed variables to $r = \frac{1}{u}$ and $L_z = r_0 v_y + r_0\Delta v_y$. Expanding this expression to leading order around the original orbit, $u = u_0 + \Delta u$, with $u_0 = 1/r_0$, and taking first-order expansions of the potential and of $L_z$, we find

$$\frac{d^2\Delta u}{d\theta^2} + \gamma^2\Delta u = -2u_0\frac{\Delta v_y}{v_y}, \tag{7.5}$$

where $\gamma^2 = \frac{u_0^2}{v_y^2}\partial_u^2\phi(u_0^{-1})$. The solution to this equation is

$$\Delta u = -\frac{2u_0\Delta v_y}{v_y}\frac{(1-\cos\gamma\theta)}{\gamma^2} - \frac{u_0\Delta v_x}{v_y}\frac{\sin\gamma\theta}{\gamma}, \tag{7.6}$$

imposing the boundary conditions that $\Delta u(0) = 0$ and $\partial_\theta u(0) = -u_0\frac{\Delta v_x}{v_y}$ (i.e., the stream particle was initially on a circular orbit and received a velocity kick, $\Delta v_x$ in the radial direction. Putting this all back in terms of $r = r_0 + \Delta r$ and expanding at leading order in $\Delta r/r_0$, we find

$$\Delta r = \frac{2r_0\Delta v_y}{v_y}\frac{(1-\cos\gamma\theta)}{\gamma^2} + \frac{r_0\Delta v_x}{v_y}\frac{\sin\gamma\theta}{\gamma}, \tag{7.7}$$

where we can put $\gamma$ back in terms of $r$ as

$$\gamma^2 = 3 + \frac{r_0^2}{v_y^2}\partial_r^2\phi(r_0). \tag{7.8}$$

Note that information about the host potential is all contained in the $\gamma$ factor.

The angular velocity of the particle is found using the conservation of angular momentum: $L_z = r^2\dot\theta$. Using our expression for $L_z$ immediately after the kick, we find

$$\begin{aligned}\dot\theta &= \frac{v_y}{r_0}\left(1+\frac{\Delta v_y}{v_y}\right)\left(1+\frac{\Delta r}{r_0}\right)^{-2}\\ &\approx \frac{v_y}{r_0}\left(1+\frac{\Delta v_y}{v_y} - 2\frac{\Delta r}{r_0}\right).\end{aligned} \tag{7.9}$$

Next, we can substitute in our expression for $\Delta r$, rearrange, and integrate to find something that involves $\theta(t)$. In detail, the result is a transcendental equation that must be solved numerically, but by doing some changing of variables and expanding at leading order, Erkal & Belokurov (2015a) arrive at

$$\Delta\theta(t) = -\frac{\Delta v_y t}{r_0}\frac{4-\gamma^2}{\gamma^2} + \frac{4\Delta v_y}{v_y}\frac{\sin\left(\frac{\gamma v_y t}{r_0}\right)}{\gamma^3} - \frac{2\Delta v_x}{v_y}\frac{\left(1-\cos\left(\frac{\gamma v_y t}{r_0}\right)\right)}{\gamma^2}, \tag{7.10}$$

which is valid as long as $\Delta\theta \ll \frac{v_y t}{r_0}$, and $\Delta\theta \ll \frac{\pi}{\gamma}$.

We can now, as a function of the initial position along the stream $\psi_0$ relative to the impact site and time $t$, predict each phase space coordinate of the stream particles.

Beginning with the stream longitude $\psi$, we find from Equation 7.10 (with a bunch of substitutions) that

$$\psi(\psi_0, t) = \psi_0 + \frac{f\psi_0 - g}{\psi_0^2 + B^2}, \tag{7.11}$$

where

$$\begin{aligned} f &= \frac{2-\gamma^2}{\gamma^2}\frac{t}{\tau} - \frac{4\sin\left(\frac{\gamma v_y t}{r_0}\right)}{\gamma^2}\frac{r_0}{v_y\tau} + \frac{2\left(1-\cos\left(\frac{\gamma v_y t}{r_0}\right)\right)}{\gamma^2}\frac{w_\parallel w_x}{w_\parallel^2}\frac{r_0}{v_y\tau}, \\ g &= \frac{2\left(1-\cos\left(\frac{\gamma v_y t}{r_0}\right)\right)}{\gamma^2}\frac{b w^2 w_z}{r_0 w_\perp^3}\frac{r_0}{v_y\tau}, \\ B^2 &= \frac{b^2+r_s^2}{r_0^2}\frac{w^2}{w_\perp^2}, \\ \tau &= \frac{w r_0^2}{2GM}, \end{aligned} \tag{7.12}$$

and $\gamma$ is as defined above. This parameterization appears quite complicated. However, note that $f, g, B, \tau$ do not depend on $\psi_0$—the mapping from $\psi_0 \to \psi$ is actually relatively simple. $\psi(t)$ in principle gives us the density profile of the stream over time: $\rho \propto \left|\frac{d\psi}{d\psi_0}\right|^{-1}$.

Erkal & Belokurov (2015a) now spend many pages of rigorously describing what this means for the behavior of the stream. We will pause here to discuss it qualitatively. From the negative sign of our expression for $\Delta v_y$, we see that the perturber tugs stream stars toward the impact site at $y = 0$. This causes an overdensity to arise at the impact site at early times, known as the "compression phase." The timescale of the compression phase is given roughly by the distance from the impact site to the particles which receive the largest kick and the largest kick velocity—$t_{\text{compress}} \sim \frac{w^3}{w_\perp^2}\frac{b^2+r_s^2}{GM}$. If this is much shorter than the timescale for a radial oscillation of the progenitor orbit $t_{\text{orb}} = \frac{r_0}{v_y\gamma}$, then the kicked particles will overtake eachother, temporarily forming a central caustic at $t_{\text{compress}}$.

The particles which the subhalo kicks along their initial orbit acquire more energy and a longer orbital period (i.e., after a while they begin to lag behind the unperturbed stream stars), while the particles kicked opposite to their initial orbit acquire a new shorter orbital period (i.e., after a while they begin to race ahead of the unperturbed stream stars). This differential streaming begins the "expansion phase," reversing the overdensity and eventually forming a gap with overdensities on either side. Erkal & Belokurov (2015a) show that the size of the gap in the density profile grows linearly in this phase, but also exhibits small oscillations due to epicyclic motions of the perturbed stars. Finally, the kicked particles experience enough differential streaming to overtake the unperturbed particles, forming caustics in the observed density profile. The rough timescale for this to occur, $t_{\rm caustic}$, is given by the leading term of Equation 7.10, where we can think of the fraction $\frac{4-\gamma^2}{\gamma^2}$ as a boost to the velocity along the stream due to slight offsets in the potential for the new orbit. Therefore, $t_{\rm caustic} \sim \frac{\gamma^2}{4-\gamma^2} t_{\rm compress}$. The outer caustic (containing the stars with the highest kick velocity) continues to expand linearly, while the new inner caustic (which sets the gap size) expands only as $\sqrt{t}$.

Figure 7.3 illustrates these phases of the perturbation, showing both a schematic of the stream position in a top-down view of the Galaxy, as well as sketches of the density profile measured by an observer at the Galactic center. See also Figure 7.4 and the hyperlinks in its caption for visualizations of stream impacts. I cannot stress highly enough how much more detail is available in §§3–5 of Erkal & Belokurov (2015a). In particular, how we might extract properties of the perturber, either from the observed density at the impact site during the compression phase/the size and central density of the gap, or the density of the peaks defining it during the expansion phase/the gap size and relative properties of the caustics during the caustic phase, or with a parametric fit to the density profile.

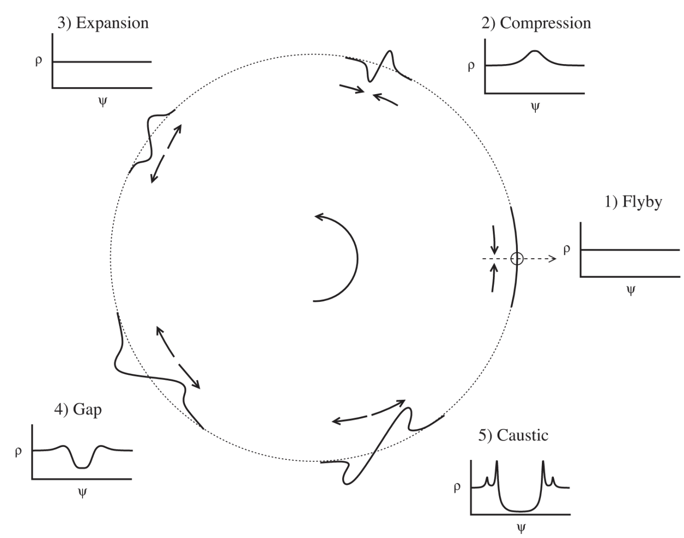


**Figure 7.3:** From Erkal & Belokurov (2015a), a schematic of the perturbation and growth of a gap in a stellar stream.

We will now turn to expressions for the other phase space dimensions of the perturbed stream particles, $(x, z)$ in addition to $\psi$ for their positions, and $(\dot{x}, \dot{y}, \dot{z})$ for their velocities.

The expression for $x$ is identical to that for $\Delta r$ derived above, since $\hat{x}$ is defined as pointing

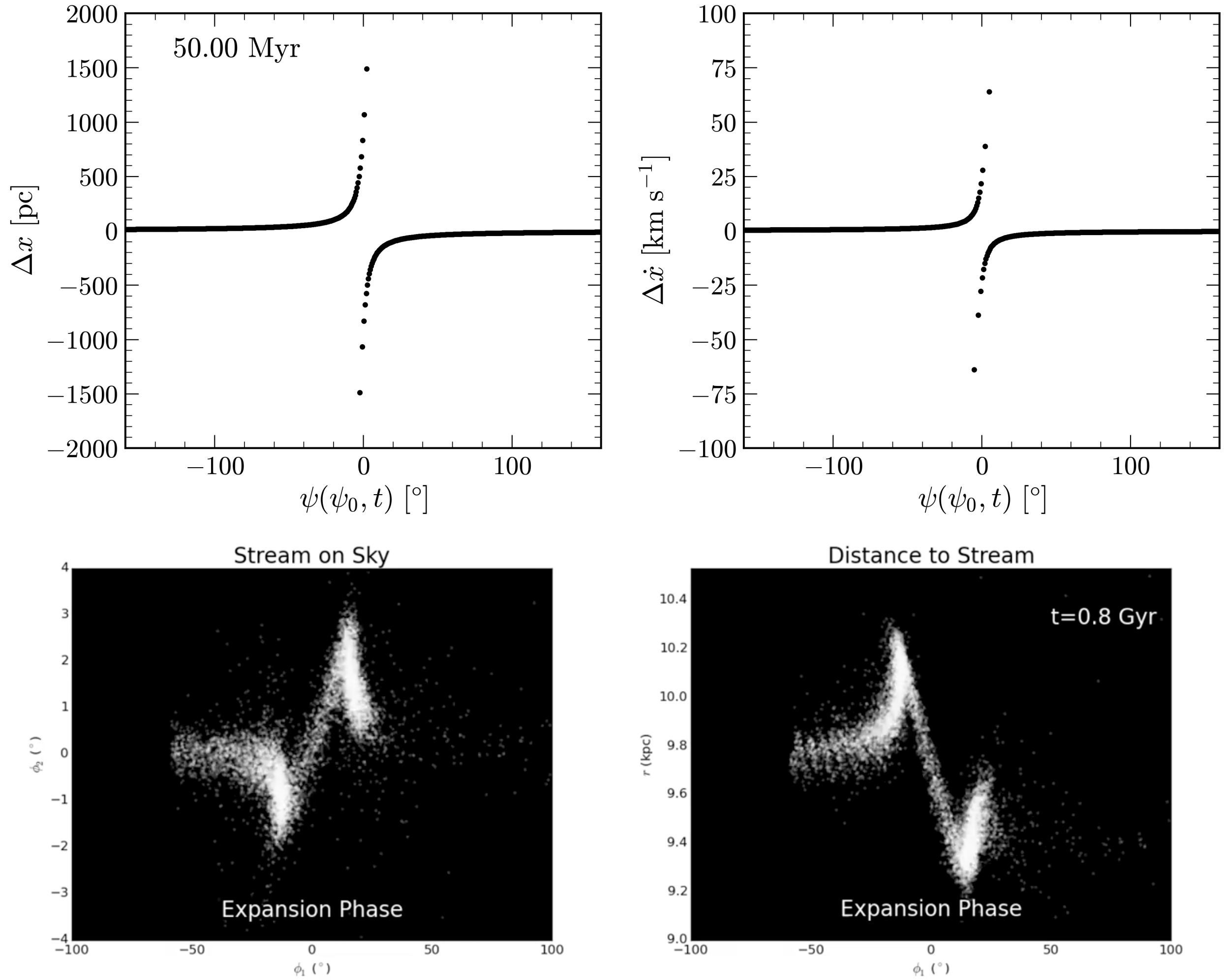


**Figure 7.4:** (Top) Simplified stream impact evolution in radial position (like Fig. 7.3 and radial velocity using the parametric expressions derived in this section, with a full movie of the impact available here. (Bottom) From Erkal & Belokurov (2015a), a stream impact for a particle spray-type stream, showing the stream latitude (left) or radial position (right) versus stream longitude, with the full movie of the impact available here.

radially away from the Galactic center:

$$\Delta x(\psi_0, t) = \frac{2r_0 \Delta v_y(\psi_0)}{v_y} \frac{2\left(1 - \cos\left(\frac{\gamma v_y t}{r_0}\right)\right)}{\gamma^2} + \frac{r_0 \Delta v_x(\psi_0)}{v_y} \frac{\sin\left(\frac{\gamma v_y t}{r_0}\right)}{\gamma}. \tag{7.13}$$

Defining $\Delta\delta_z \equiv \frac{\Delta z}{r_0}$ as the stream latitude ("$\phi_2$" in most other work, where the longitude coordinate would be $\phi_1$, except that here we're already using the symbol $\phi$ to represent the host potential unfortunately), we find

$$\Delta\delta_z(\psi_0, t) = \frac{\Delta v_z(\psi_0)}{v_y} \sin\left(\frac{v_y t}{r_0}\right). \tag{7.14}$$

This is the oscillatory motion mentioned above, which is the same motion described by the epicycle approximation in Chapter 5.

Taking a time derivative of $\Delta x(t)$, we find

$$\Delta\dot{x}(\psi_0, t) = \frac{2\Delta v_y(\psi_0)}{\gamma} \sin\left(\frac{\gamma v_y t}{r_0}\right) + \Delta v_x(\psi_0) \cos\left(\frac{\gamma v_y t}{r_0}\right) \tag{7.15}$$

for the radial velocity.

The velocity along the stream is given by

$$\Delta\dot{y}(\psi_0, t) = (r_0 + \Delta x(\psi_0, t))\dot{\theta}(\psi_0, t) - v_y, \tag{7.16}$$

where $\dot{\theta}(\psi_0, t)$ was derived above.

Finally, we take the time derivative of the offset along $z$ to find

$$\Delta\dot{z}(\psi_0, t) = \Delta v_z(\psi_0) \cos\left(\frac{v_y t}{r_0}\right). \tag{7.17}$$

We are left with six observables: $(\psi(\psi_0, t), \Delta x, \Delta\delta_z, \dot{x}, \dot{y}, \dot{z})$, but seven model parameters $(M, r_s, w_x, w_y, w_z, b, t)$. This means that in the best case scenario we can determine the parameters only up to a 1-D degeneracy. Erkal & Belokurov (2015b) devote again, *many* pages to exploring this degeneracy and which parameters can be obtained from various subsets of the observables. The upshot is an unavoidable degeneracy between the perturber's mass and its velocity.

Note: Action-angle descriptions of stream perturbations exist, and I have neglected to read those papers for now, but some examples are Sanders et al. (2016); Bovy et al. (2017).

How do we apply this in practice? With exactly the equations we have now, we can construct a likelihood of each observable given some set of model parameters, then take many samples of model parameters and do MCMC to find their posterior. See §4 of Erkal & Belokurov (2015b).

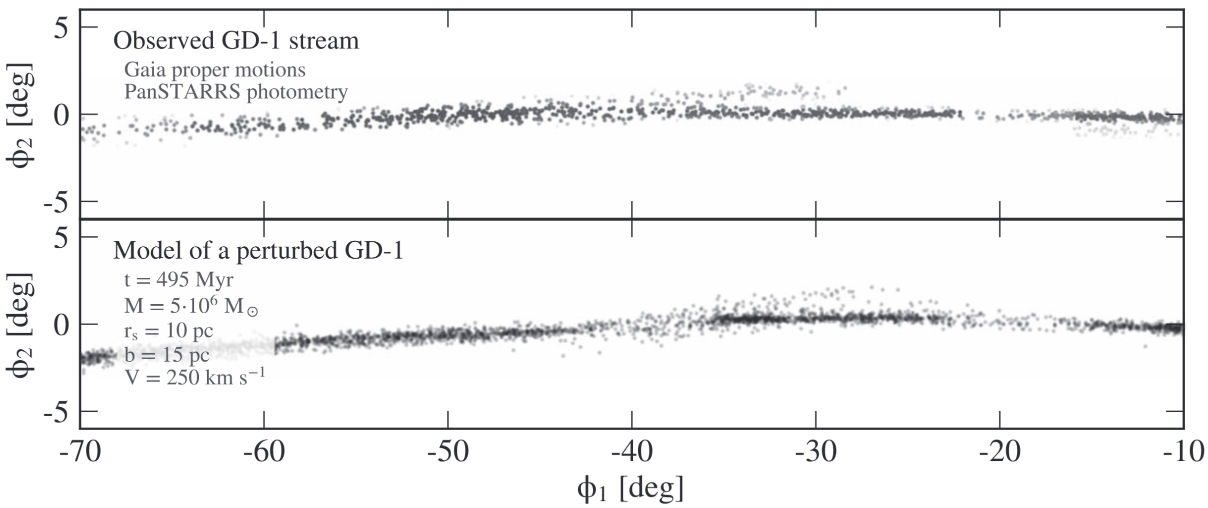


Let's take Ana's studies of the perturbed region of the GD-1 stellar stream as an example. GD-1 is famous for its density variations and spur feature which are attributed to perturbations from small scale Milky Way structure (see above). Bonaca et al. (2019) use only positions from *Gaia* to constrain the allowed impact geometries, perturber properties, and impact time that created the spur/gap. See the corner plot in Figure 7.5. Using the allowed impact times and impact parameters, Bonaca et al. (2019) are able to show that no luminous perturber with a known orbit passed close enough to create the observed feature. Further, with the allowed masses and sizes of the perturber, they show that the density of the perturber is not consistent with giant molecular clouds (which may otherwise have been candidates, as they are present when the stream passes through the Galactic disk). Radial velocities further constrain the impact properties in Bonaca et al.

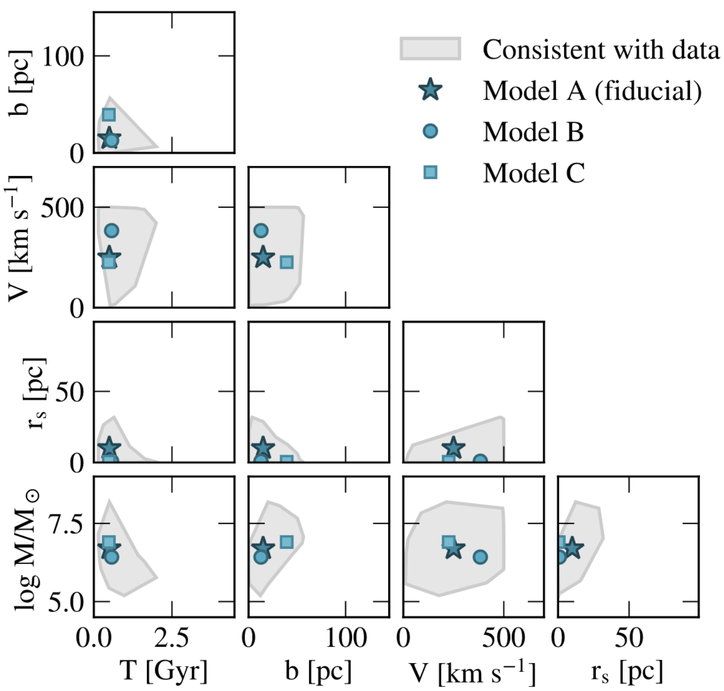


**Figure 7.5:** From Bonaca et al. (2019).

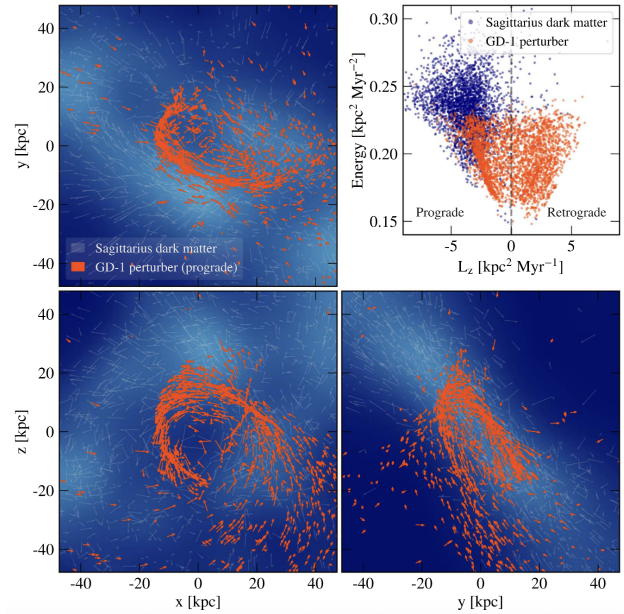


**Figure 7.6:** From Bonaca et al. (2020), allowed present day locations of the GD-1 perturber.

(2020), such that they may map the allowed present day locations of the perturber, which overlap the Sagittarius stream (see Figure 7.6). The implication here is that a dark matter subhalo from the Sagittarius dwarf galaxy is the GD-1 perturber, though the current precision limitations on the proper motions from *Gaia* inhibit further localization.

---

We now turn to the bigger picture of the feasibility of detecting subhalo impacts across MW streams.

Lu et al. (2025) use the framework from Erkal & Belokurov (2015a,b) to prescribe a test for the minimum detectable subhalo mass given the properties of a stream and the quality of available observations. Note that their methods assume a stream on a circular orbit in the plane of the disk and *an observer located at the Galactic center*. The first step is to determine the intrinsic dispersions in the stream star positions, velocities, and density variations. These come from the recipe for particle spray streams in Fardal et al. (2015), where

$$\begin{aligned} \sigma_r \propto \sigma_z \propto r_{\rm tid} \\ \sigma_{v_r} \propto \sigma_{v_t} \propto \sigma_{v_z} \propto r_{\rm tid}/r_0. \end{aligned} \tag{7.18}$$

Here we have redefined $(x, y, z) \to (r, t, z)$, $r_0$ is the radius of the orbit, and $r_{\rm tid}$ is the progenitor's tidal radius, which we learned about in Chapter 4:

$$r_{\rm tid} \propto \left(\frac{M_{\rm prog}}{r_0}\right)^{1/3} r_0 \tag{7.19}$$

(at least for a simplified logarithmic potential, where $M_{\rm enc}(< r_0) \propto r_0$). Fundamentally, the intrinsic internal stream dispersions are governed by the progenitor mass and the size of the orbit $r_0$. Note that $\sigma_z = r_0\sigma_\theta$ for angular stream width $\sigma_\theta$, so that for a given $r_0$, the stream width and progenitor mass directly correspond.

The actual error on the mean of quantity $X$ for the subset of $n$ stream stars that we observe is $\sigma_{\overline{X}} = \sigma_x/\sqrt{n}$, which in turn depends on the intrinsic density of stars in the stream, characterized by $\lambda$, or the number of stars per unit angle. Directly from Fardal et al. (2015),

$$\lambda = \frac{4}{3}\frac{N_{\rm stars}}{l} \tag{7.20}$$

for a stream of total length $l$ with $N_{\rm total}$ observed stars total. Given the ($\sim$measurable) stellar mass of the stream plus the initial mass function, we can determine $N_{\rm stars}$ from observations, so $\lambda$ corresponds directly with $M_{\rm stellar}$.

To generate realizations of subhalo impacts, Lu et al. (2025) find the value of the analytic model in 2° bins along the stream to get the expected value of the observables in each bin, then draw the observables $X$ of the stream stars in the bin from a Gaussian with error $\sigma_{\overline{X}}$ given the stream's parameters $(\sigma_\theta, r_0, \lambda)$.

Next, they apply observational effects for several "benchmark scenarios" (e.g., *Gaia* photometry and astrometry + DESI radial velocities, *Gaia* astrometry + LSST photometry + Via radial velocities, etc; see their §3). Each simulated survey imposes a magnitude limit, so that the number of observable stars changes. The first effect of this is to increase the Poisson noise in the number density uncertainty in each bin. The effect for the position uncertainties is similar. The velocity uncertainties vary from star to star since they are magnitude dependent, so the expected value and variance have slightly different expressions when accounting for observational effects (they now include both $\sigma^2_{X,\rm disp}$ and $\sigma^2_{X_i,\rm obs}$ terms for the intrinsic stream dispersion as applied to all stars and the observational uncertainty for the $i^{\rm th}$ star, respectively). The magnitude dependence in the RV and proper motion uncertainties come directly from each survey's documentation (or in the case of Via, from "V. Chandra, private communication").

The expected values and variances of the binned mock data can all be folded together into a likelihood function

$$L(M_{\rm sh}, \boldsymbol{\theta}) = \prod_{i,j} \frac{1}{\sqrt{2\pi\sigma^2_{\nu_{i,j}}}} \exp\left[-\frac{(\nu_{i,j}(M_{\rm sh}, \boldsymbol{\theta}) - \nu^{\rm dat}_{i,j})^2}{2\sigma^2_{\nu_{i,j}}}\right], \tag{7.21}$$

for subhalo mass $M_{\rm sh}$ and other impact model parameters $\boldsymbol{\theta}$. $\nu_{i,j}$ are the analytically-predicted value of the $i^{th}$ observable for the $j^{th}$ bin along the stream, with the superscript

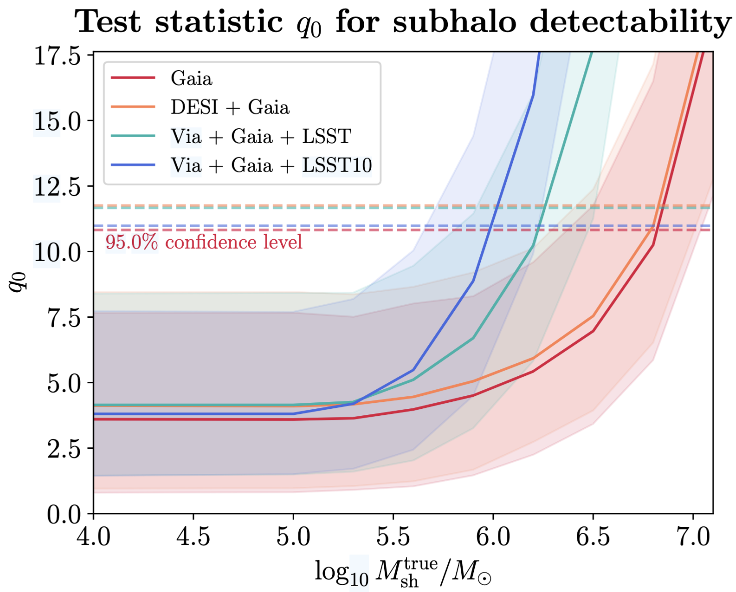


**Figure 7.7:** From Lu et al. (2025)

'dat' version (and the variance terms) coming from the mock impacts generated with intrinsic stream dispersions + observational uncertainties. In order to establish a threshold for "detection," Lu et al. (2025) now define a test statistic

$$q_0 = 2 \ln \frac{L(\hat{M}_{\rm sh} \hat{\boldsymbol{\theta}})}{L(0)}, \tag{7.22}$$

where the quantities with hats are the impact model parameters that maximize the likelihood function (literally just using `scipy.optimize`! huge numerical methods moment), and $L(0)$ is the likelihood of a model where there is no impact. A "detection" at the 95% confidence level occurs when $q_0$ exceeds the 95th percentile of the $q_0$ distribution where $M_{\rm sh}^{\rm true} = 0$ (which we get from generating many "no impact" realizations). Figure 7.7 shows $q_0$ as a function of subhalo mass for four observational scenarios, marking the 95% confidence levels in each case so that we can read off the minimum detectable subhalo masses. The shaded regions are the $\pm 1\sigma$ variation from 500 realizations of mock data at each subhalo mass.

Now we just repeat for different stream properties! That result is in Figure 7.8, where the panels show the minimum detectable subhalo mass varying one stream parameter (width, galactocentric distance, stellar density) at a time. The dashed lines are from power laws fit to this data in each observational scenario, which provide direct formulas for the minimum detectable subhalo mass given stream properties!

Lu et al. (2025) also define confidence intervals on the detected subhalo mass based on another test statistic; I am omitting that discussion from this summary.

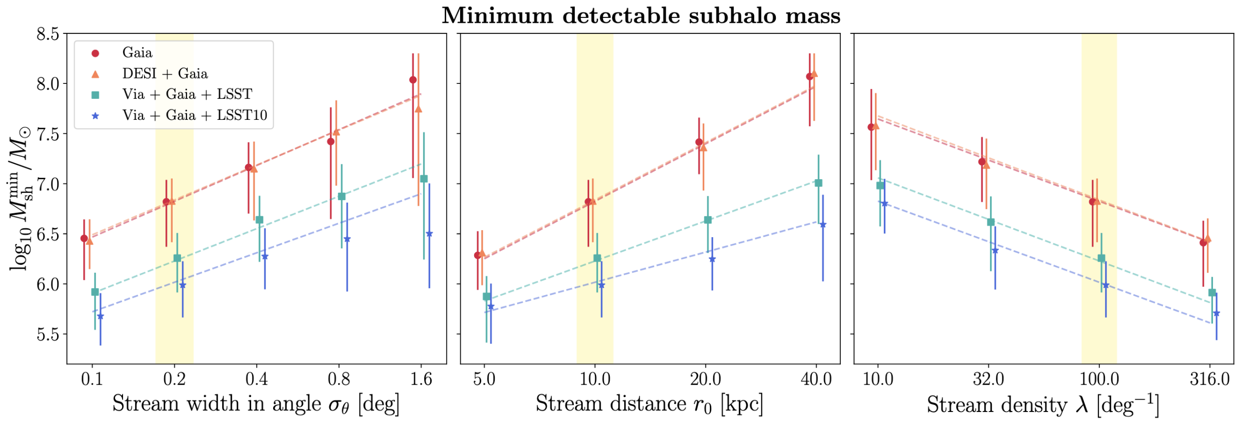


**Figure 7.8:** From Lu et al. (2025)

They also experiment briefly with the effect of the length of the stream $l$ on subhalo detectability, since shorter streams capture a smaller fraction of the full perturbation profile leading to higher mass detection thresholds. They find, though that there are diminishing returns for streams of angular lengths $\Delta\psi \gtrsim 16°$. They impose that a stream must be $\gtrsim 20°$ long in searching actual MW streams (in order to be able to avoid using the region of the stream near the progenitor or the very ends of the tails).

Finally, they explore the effect of the remaining "nuisance" parameters of the perturbation; the impact parameter, the time since the impact, the magnitude and direction of the subhalo velocity, and the mass/scale radius relation for the subhalo. Figure 7.9 shows the results that exploration, where the main point is that the highlighted values used to create the function for minimum halo mass from stream properties are basically representative of all impacts:

- The impact parameter does not drastically change the detectability until it becomes much larger than the thickness of the stream
- As we vary the time since the impact, the detectability jumps around a bit (due to the different phases/oscillatory nature of the gap growth we saw earlier).
- There is little dependence of the detectability on the direction of the impact, unless the velocity is mostly tangential (in which case the relative velocity shrinks and the effective impact duration gets longer, amplifying the signal).

While variations in the concentration are explored briefly here, for the most part this paper assumes a fixed subhalo concentration (mass/scale radius relation) from CDM.

Now Lu et al. (2025) are equipped to rank every known stream in the Milky Way by the minimum mass of subhalo that could be detected based on these methods. They use the

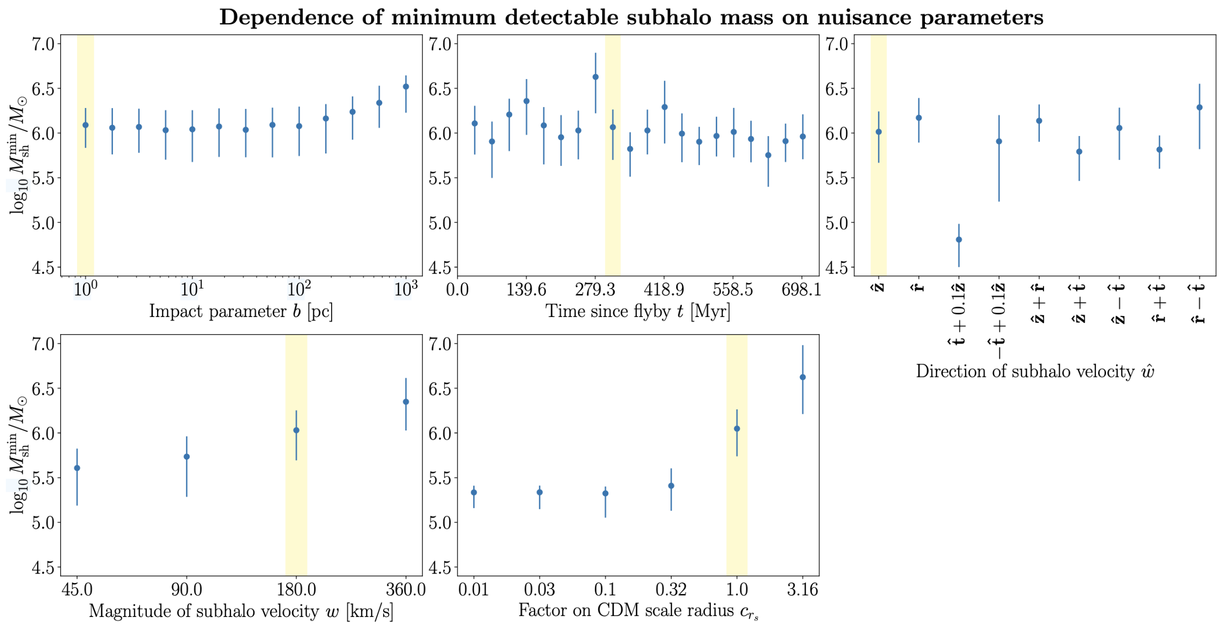


**Figure 7.9:** From Lu et al. (2025). The highlighted values are the defaults used to create the relation for minimum detectable subhalo mass as a function of stream parameters.

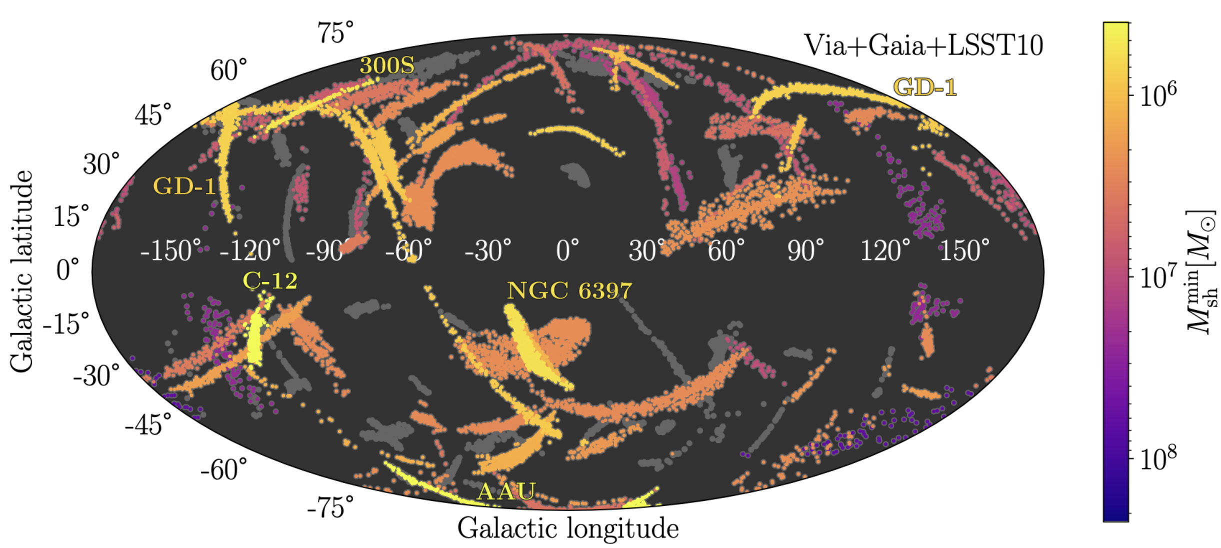


**Figure 7.10:** From Lu et al. (2025).

stream widths, lengths, and heliocentric distance $r_h$ (in place of $r_0$) from Bonaca & Price-Whelan (2025), keeping only streams with reported stellar masses, lengths $> 20°$, and stellar densities $\lambda \geq 1$ per $2°$. For the best-case observational scenario, the minimum halo mass detectable using each stream is shown in Figure 7.10 (and as a long table in their paper).

The ranking of MW streams by minimum detectable halo mass is exciting but somewhat limited:

- The observer has been assumed to be located at the galactic center, so that $r_0$ contributes both to the cluster's tidal radius (and thus the intrinsic stream properties) *and* the observability, since it controls the observer's distance to the stream as well. In reality, I think these two effects should be less coupled. The shapes of perturbations also change with viewing angle–a good chunk of the Lu et al. (2025) is dedicated to the "relative importance" of different observables to the subhalo detectability (in terms of their contributions to the likelihood), but these rankings depend on viewing the stream from the Galactic center. For example, the default impact geometry for this work, radial velocities are ranked as relatively unimportant to detectability when viewing the stream from the Galactic center.

- The threshold for detectability should in principle also depend on our ability to model the progenitor orbit (since perturbations are measured relative to the baseline stream track). An eccentric orbit complicates this calculation.

- This work neglects any non-subhalo gravitational influencers of the stream besides a simple logarithmic external MW potential, but we have seen that individual MW streams are known to show extra perturbations from the bar/Magellenic clouds/etc.

- The assumptions for the intrinsic stream observable dispersions ultimately depend on how much you trust the Fardal et al. (2015) particle spray recipe. E.g., stellar mass (and hence, observability) dependence along the stream due to mass segregation in the progenitor is not modeled.

- The subhalo mass-radius relation has been fixed to the prediction of CDM, which breaks the degeneracy we mentioned earlier between the subhalo's mass and the encounter speed. An alternative approach involves doing a full orbit integration of the mock stream in the presence of a subhalo (and using a non-Plummer subhalo profile), which lets us leave the subhalo scale radius as a free parameter, but is much more expensive.

This work is meant as a first-order approach to prioritizing future observations of MW streams when looking for subhalo impacts, even if there are caveats and complications.